https://doi.org/10.1016/j.applthermaleng.2016.11.040

Flame Propagation of Premixed Liquefied Petroleum Gas Explosion in a Tube

(Abbreviated title: Flame Propagation of LPG Gas Explosion)

Y. Huo
College of Aerospace and Civil Engineering
Harbin Engineering University
Harbin, Heilongjiang, China

W.K. Chow*
Department of Building Services Engineering
The Hong Kong Polytechnic University
Hong Kong, China

*Corresponding author:
Fax: (852) 2765 7198; Tel: (852) 2766 5843
Email: beelize@polyu.edu.hk; bewkchow@polyu.edu.hk
Postal address: Department of Building Services Engineering, The Hong Kong Polytechnic University, Hunghom, Kowloon, Hong Kong.

Submitted: June 2016
Revised: August 2016
Further revised: September 2016

Abstract

Flame propagation in premixed liquefied petroleum gas (LPG) explosion was studied experimentally in a tube of diameter 2.6 m and length 25 m. Experiments on LPG explosion were conducted in a single zone first in this large explosion tube. The explosion tube was then divided into two zones with different mixing ratios of LPG and air. A thin polyvinyl chloride (PVC) film sheet was used to adjust the length of each zone. A total of three single-zone experiments and five two-zone experiments were carried out. Explosion phenomena and flame propagation in the tube were studied analytically using experimental results and theoretical analysis. A simple model for the flame propagation was proposed and tested using the experimental data in the present study and some literature results. Flame propagation characteristics were found with a general trend to vary with time as an exponential function for adequate fuel with uniform concentrations within a certain distance of the tube. The flame propagation speed at a point in explosion depends on the turbulent burning speed and expansion ratio. Experimental data deviated more from the empirical exponential function for larger variations of fuel concentrations.

Keywords: Premixed fuel gas, explosion, flame propagation, tube experiment

1. Introduction

Liquefied petroleum gas (LPG) is widely used as fuel in the Asia-Oceania region with 22,000 LPG taxis and minibuses in Hong Kong [1]. Fire risks associated with LPG vehicle systems were reported by Chamberlain and Modarres [2], suggesting that LPG buses are 2.5 times more prone to fire fatality risk than diesel buses. An explosion in an LPG taxi occurred [3] in Hong Kong. Explosions of clean refrigerants with chemical compositions similar to LPG in environmental friendly air-conditioning systems have also been reported [4,5]. Therefore, LPG explosion should be studied more thoroughly because of the emerging popularity of LPG in transport and of the severity in case of explosion.

Large-scale explosion experiments require large amounts of resources but the repeatability is low. Explosion experiments [6-8] of fuel gas were then carried out in tubes. A 21 m long steel piping with an inner diameter of 110 mm with stoichiometric hydrogen-air mixture explosion was studied by Hajossy and Morva 1998 [9]. Transient flame spread can be approximated by cubic-spline polynomials. Chatrathi et al. 2001 [10] studied tubes of diameter 0.1524 m, 0.254 m and 0.4064 m with propane, ethylene and hydrogen explosion. The effects of the diameter, fuel type and tube structure on flame propagation in explosion were studied. For tube with a length-to-diameter ratio greater than 50, flame velocity increased with tube diameter. Premixed laminar flames accelerating in tubes were reported by Bychkov et al. [11-13]. Xiao et al. 2014 [14] studied experimentally premixed hydrogen/air flame propagation in a partially-open duct of 82 mm x 82 mm square section and 530 mm long. Results indicated that the tube opening ratio would affect flame propagation in explosion. Flame propagation increased with time as an exponential function. Hisken et al. 2015 [15] studied propane-air gas explosion experiments in two vented channels of dimensions 1.5 m × 0.3 m × 0.3 m in laboratory scale and 6 m × 1.2 m × 1.2 m in medium scale. Yu et al. 2015 [16] investigated the effects of hydrogen addition on the fundamental characteristics of propagating premixed methane/air flames at different equivalence ratios in a horizontal duct of cross-sectional area 150 × 150 mm^2 and length 1000 mm. Also, Yu et al. 2015 [17] studied hydrogen/methane deflagration of premixed flame in a tube less than 1 m long.

Experiments were carried out in a much larger tube of cross-sectional area 7.2 m^2 and length up to 896 m in China by Cai et al. [18]. Such experiments provided valuable experimental explosion data. However, understanding of explosion flame front propagation with distance is still limited.

It is common practice to put barriers in the experimental tube to study flame spread. Johansen et al. 2009 [19] studied the effect of blockage ratio on the early phase of the flame

acceleration process in a tube of length 2.44 m and square section 7.6 cm × 7.6 cm. Luo et al. 2010 [20] conducted gas deflagration experiments and modeled flame propagation speed experimentally in a tube of diameter 0.08 m and length 5.26 m with barrier, called horizontal semi-open deflagration tube. Analytical expressions on the premixed flame acceleration induced by wall friction in two-dimensional channels and cylindrical tubes were studied by Demirgok et al. 2015 [21].

Flame spread in a curved explosion tube was studied by Robert et al. 2010 [22] with propane, ethylene and hydrogen-air explosion. Experiments were carried out in an 18 m long DN150 closed pipe with a 90^{o} bend and various baffle obstacles placed at a short distance from the ignition source. Emami et al. 2013 [23] studied experimentally the flame propagation of hydrogen/air and hydrogen-methane/air mixtures in a 90° bend pipeline. Emami et al. 2016 also [24] studied the effect of tube structure on flame propagation in explosion in a tube of diameter 0.1 m.

Deflagration and then detonation experiments in a tube were studied by Valiev et al. 2013 [25]. The phenomenon of spontaneous acceleration of a premixed flame front propagating in micro-channels was studied, with subsequent deflagration-to-detonation transition. Wang et al. 2015 [26] investigated flame acceleration and deflagration-to-detonation transition (DDT) in a steel duct 24 m long and 80 mm by 80 mm in square cross-section, with arrayed obstacles.

There were not many experiments on large-scale explosion, probably due to resources limitation. A brief review on experiments carried out in explosion tube with diameter over 1 m is listed in Table 1.

In this paper, flame propagation characteristics in LPG explosion in a tube of diameter 2.6 m and length 25 m will be reported. LPG was purchased from the market with about 60% of propane (C_3H_8) and 40% of butane (C_4H_{10}), with a small amount of propene (C_3H_6) and butene (C_4H_8), and additives. Both single-zone and two-zone experiments with different LPG-air mixing ratios were carried out. All these experiments were conducted in tubes of small diameter. Very few experiments were with diameter over 2 m. Most of the tests were on single zone, not divided into different zones. Two-zone experiments were carried out to simulate situations with non-uniform distribution of fuel gas concentrations.

2. Modelling Explosion in Long Tubes

Explosion in a long tube of radius R can be analyzed using a one-dimensional model as shown in Fig. 1. One end of the tube is closed with the other end open. The x-direction for flame propagation is taken to be along the tube from the closed end. The premixed fuel concentration was assessed to be adequate for combustion, and the flame surface would fill up the entire tube cross-section. The flame surface is taken as a cylindrical surface of radius r, which is approximately equal to R, for tubes with a small diameter.

Taking ρ_{u} to be the density of fuel gas mixture and S_{u} to be the speed of fuel gas supply at the flame front, the mass of fuel gas Δm consumed by the flame in time Δt can be written in terms of the flame surface area A as:

$$\Delta m = AS_u \rho_u \Delta t \tag{1}$$

For tubes with a small diameter, the area of the circular flame front can be ignored compared with the curved cylindrical surface. But for tubes with a larger diameter, flame surface area A has two parts (assuming $r = R$):

$$A = 2\pi Rx + \pi R^2 \tag{2}$$

Let the increase in fuel gas product volume be ΔV, then the increase in mass is $\rho_{\mathrm{b}}\Delta V$, where ρ_{b} is the density of fuel gas product. Using mass conservation:

$$\frac{\Delta V}{\Delta t} = \frac{\mathrm{d}V}{\mathrm{d}t} = \left(2\pi Rx + \pi R^2\right) S_{\mathrm{u}} E \tag{3}$$

In the equation above, the expansion ratio E is given by $\rho_{\mathrm{u}}/\rho_{\mathrm{b}}$. It should be pointed out that both S_u and E are taken to be constants for simplicity. A more rigorous approach to give the flame propagation speed S_u is given later in section 6.

As $V = \pi R^2 x$, putting into the ordinary differential equation (3) and solving it gives:

$$x = \mathrm{C}\exp\left(\frac{2ES_{\mathrm{u}}}{R}t\right) - \frac{R}{2} \tag{4}$$

In equation (4), C is a coefficient which depends on the initial conditions of fuel gas explosion. Experimental studies in the following sections were carried out to justify the acceptability of this model.

3. Experimental Studies with a Long Tube

A tube of diameter 2.6 m and length 25 m as in Fig. 2(a) was constructed for explosion experiments using 10 mm thick steel plates in a remote site at Lanxi, Harbin, Heilongjiang, China. There were support fitting rings at every 1 m interval for installing thin films or thick sheets. The explosion tube can then be partitioned into different lengths or with different arrangements of combustion chambers. Four observation windows of 0.8 m diameter were available along one side of the tube.

Different experimental lengths or chambers were partitioned out from the tube using thin plastics films or polyvinyl chloride (PVC) sheets of 1 mm thick. The cross-sectional area of the tube was 5.3 m^2. (Fig. 2(b) and (c))

LPG was used as the fuel gas in all explosion experiments. The combustion chamber was filled up with the fuel gas with the concentration checked. The mixing ratio of fuel gas was ensured by operating a circulating pump for 30 minutes. Up to 8 flame detectors were installed with data saved in a data logger at a sampling time of 0.2 ms.

In the single-zone experiments (Fig. 2(b)), three sets of experiments (S1-S3) using a tube length of 25 m were carried out, with LPG gas-to-air ratio of 6%:

- S1: Tube partitioned to form a zone of length 1 m by plastics thin film, containing LPG-air mixture volume of 5.3 m^3.
- S2: Tube partitioned to form a zone of length 2 m by plastics thin film, containing LPG-air mixture volume of 10.6 m^3.
- S3: Tube partitioned to form a zone of length 3 m by plastics thin film, containing LPG-air mixture volume of 15.9 m^3.

In the two-zone experiments, two PVC sheets were inserted to give two combustion chambers containing premixed LPG gas with different concentrations for experiments using tube portions of length 11 m and 16 m, as shown in Fig. 2(c). Premixed LPG at gas-to-air ratio of 6% was stored in combustion chamber A and the gas was ignited by a high-voltage electric spark igniter (2 × 4 kV 20 mA). The other chamber B was filled up with LPG at gas-to-air ratio of 10%. No ignitor was installed in chamber B, and gas was ignited in chamber B due to the explosion in chamber A.

Five sets of experiments (D1-D5) with two zones were carried out:

- D1: Tube length 11 m, partitioned by plastics thin film into chamber A of length 2 m containing a volume of 10.6 m^3 LPG-air mixture, and chamber B of length 5 m containing a volume of 26.5 m^3 of LPG-air mixture.
- D2: Tube length 11 m, partitioned by plastics thin film into chamber A of length 3 m containing a volume of 15.9 m^3 LPG-air mixture, and chamber B of length 4 m containing a volume of 21.2 m^3 of LPG-air mixture.
- D3: Tube length 11 m, partitioned by plastics thin film into chamber A of length 4 m containing a volume of 21.2 m^3 LPG-air mixture, and chamber B of length 4 m containing a volume of 21.2 m^3 LPG-air mixture.
- D4: Tube length 16 m, partitioned by plastics thin film into chamber A of length 2 m containing a volume of 10.6 m^3 LPG-air mixture and chamber B of length 3 m containing a volume of 15.9 m^3 of LPG-air mixture.
- D5: Tube length 16 m, partitioned by plastics thin film into chamber A of length 3 m containing a volume of 15.9 m^3 LPG-air mixture, and chamber B of length 4 m containing a volume of 21.2 m^3 LPG-air mixture.

A summary of these tests is shown in Table 2.

4. Experimental Results

All staff members were asked to stay away from the explosion tube during the experiments. Safe workplaces were assigned to observe the flame movement. Video cameras were housed at appropriate positions to take photographs and videos of explosion. Flame shapes and gases coming out from the openings were also observed and recorded.

For single-zone experiments S1 to S3, flame fronts and flame shapes upon igniting the LPG gas mixture in different zone size were clearly observable through the windows as the tube environment was darker. Large amounts of gases were observed to be moving out of the open end of the explosion tube. However, flame shapes outside the tube were not clearly observable due to background lighting. Loud noise due to explosion was heard. The tube itself vibrated due to recoil momentum generated from explosion, moving in opposite direction to the gas motion.

For experiments with two zones D1 to D5, flame fronts and flame shapes at different positions inside the tube were also clearly observable through the windows, upon igniting the LPG gases. Large amounts of gases were observed to be moving out of the open end of the explosion tube. Very bright yellow flames moved out of the tube to 10 m beyond the opening. The flame outside the tube was clearly observable even under bright background lighting. The flames tended to move up due to buoyancy of the accompanying hot gases. Different conditions of the two zones resulted in different flame movement patterns inside the tube and flame shapes outside. Again, loud noise was generated due to explosion but with a lower pitch. The tube itself vibrated due to recoil momentum generated from explosion, moving in opposite direction to the gas motion. Although the flame movement distance inside the tube for the two-zone experiments were shorter than that of the single-zone ones, stronger explosion resulted. The recoiled momentum acting at the explosion tube was much larger, resulting in very strong vibrations.

The flame patterns at the open end for the two-zone explosion experiments D2 and D5 are shown in Fig. 3. Experiments D2 and D5 were carried out in the tubes of effective length 11 m and 16 m respectively. The ignition chamber A had a length of 3 m and an LPG gas-to-air ratio of 6%. Chamber B had a length of 4 m and a gas-to-air ratio of 10%.

Flame was observed at the open end with pictures taken shown in Fig. 4. The interior part of the tube was rich in fuel, and not burnt out completely. Unburnt fuel moved out of the tube, mixed with air and burnt to give the flame. From the pictures, flame observed at the upper end as the cross-sectional area of the tube was large. Hot flame stayed at the upper part due to buoyancy first, then moved down the tube to mix with air and then burnt. Under all experimental conditions, LPG concentration in the tube would be adequate to sustain combustion with flame surface fill up the tube cross-section.

5. Analysis

Flame propagation speed and expansion factor are very complex and not describable by simple relations. To modify the results obtained in the simple model proposed, equation (4) is written in terms of two coefficients C_1 and C_2 as:

$$x = C_1 \exp(C_2 t) - \frac{R}{2} \tag{5}$$

Numerical values of C_1 and C_2 can be deduced from experiments.

Flame front locations at different times for the explosion experiments are shown in Fig. 5. Results appear to agree with equation (5). Coefficients C_1 and C_2 can be found from fitting and compared with LPG gas-to-air ratios in chambers A and B.

In single-zone experiment S3 with a 25 m long tube, and two-zone experiment D5 with a 16 m long tube, flame speed S_u at different locations x are plotted in Fig. 6. Flame speed increased slowly initially for both experiments S3 and D5, but the curve shapes for S_u are different as explosion developed. For single-zone test S3, S_u increased when x is over 3.5 m and kept rising until 5 m as tube walls limited flame development along the radial direction. Burning up fuel vapour would slow down the rising rate of S_u.

For two-zone experiment D5, S_u increased sharply at 4.5 m, then reduced suddenly, but increased again at 12 m. That is because the fuel concentrations are different along the longitudinal direction x of the tube. Changes in flame speed due to regional distribution of concentration will be discussed later in section 6.

Literature results [8, 27] on explosion tube experiments are extracted for comparison with those in the present study. In a tube of length 8.25 m, and rectangular cross-section of 2.8 m by 3 m using methane (CH_4) and hydrogen (H_2) at different ratios, flame front propagation in Fig. 7 indicate results (Lowesmith et al. 2011) in agreement with equation (5). Similar observations (Wang et al. 2010) were obtained for a 200-m long tube of diameter 2.5 m using methane (Fig. 8).

The experimental results reported in the literature [8,27] and observed in the present study on explosion tube are summarized in Tables 2 and 3 with regression coefficient γ^2 shown. It is observed that equation (5) gives a reasonable description of the instantaneous positions of the flame front. Even at premixed LPG concentration of 6% and 10% with barrier in the explosion tube, equation (5) agrees fairly well with experiments.

However, equations (3) and (4) were obtained under the assumption that the explosion flame propagated with E and S_u regarded as constant in time. This is different from reality. Experimental results indicated that flame front developed in the tube with an exponential function within a certain distance. However, the constant S_u describes only the time-averaged flame speed, not the actual instantaneous speed. Thus, equation (4) can only give a general trend of flame front locations at different times. A more detailed derivation is presented in the next section by taking the instantaneous flame front speed as S_F, to distinguish it from S_u.

6. Flame Front Speed

Following the analysis of flame front propagation speed [28] without considering the initial velocity S_I of the gases, explosion in the tube can be described by the burning velocity S_C, velocity component S_N due to change in the number of moles in the burning process, and gas-expansion velocity S_E due to thermal heating.

$$S_C = S_{Lr}\left(\frac{T}{T_r}\right)^{\alpha}\left(\frac{p_r}{p}\right)^{\beta} \tag{6}$$

$$S_N = S_{Lr}\left(\frac{T}{T_r}\right)^{\alpha}\left(\frac{p_r}{p}\right)^{\beta}\left(\frac{\overline{M}_u}{\overline{M}_b}-1\right) \tag{7}$$

$$S_E = S_{Lr}\left(\frac{T}{T_r}\right)^{\alpha}\left(\frac{p_r}{p}\right)^{\beta}\frac{(T_b-T)}{T}\frac{\overline{M}_u}{\overline{M}_b} \tag{8}$$

$$S_F = S_{Lr}\left(\frac{T}{T_r}\right)^{\alpha}\left(\frac{p_r}{p}\right)^{\beta}\frac{T_b}{T}\frac{\overline{M}_u}{\overline{M}_b} \tag{9}$$

A detailed derivation of the above equation is shown in the Appendix. Here S_F is the flame front speed and S_{Lr} is a reference speed.

In view of equations (6) to (9), S_N, S_E and S_F depend on S_C. Equation (6) on S_C is derived using laminar flow. In practical cases, S_C commonly depends on turbulence intensity r'_{rms} too:

$$S_C = S_L + Kr'_{rms} \tag{10}$$

In the equation above, S_L is the flame front speed in laminar flow and K is a coefficient which depends on flow structure and burning fuel. As shown in Fig. 9, assuming chemical reactions occur only at the flame surface, taking S_C as $S_L + Kr'_{rms}$, and taking the flame surface motion due to turbulence to be S_T, then S_T and S_L would satisfy:

$$S_T \propto S_L\left(\frac{r'_{rms}}{S_L}\right) \tag{11}$$

In this way, the explosion flame burning speed is close to the average turbulent burning speed, and equations (6) to (9) become:

$$S_C = S_T \tag{12}$$

$$S_N = S_T\left(\frac{\overline{M}_u}{\overline{M}_b} - 1\right) \tag{13}$$

$$S_E = S_T \frac{\left(T_b - T_u\right)}{T_u}\frac{\overline{M}_u}{\overline{M}_b} \tag{14}$$

$$S_F = S_T \frac{T_b}{T_u}\frac{\overline{M}_u}{\overline{M}_b} \tag{15}$$

From $m_u = V_u\rho_u$ and $m_b = V_b\rho_b$, the expansion ratio becomes:

$$E = \frac{m_u V_b}{V_u m_b} \tag{16}$$

Substituting for volume from the ideal gas law,

$$p_b V_b = \frac{m_b}{\overline{M}_b}\Re T_b \tag{17}$$

$$p_u V_u = \frac{m_u}{\overline{M}_u}\Re T_u \tag{18}$$

gives:

$$\frac{V_b}{V_u} = \frac{\overline{M}_u T_b P_0}{\overline{M}_b T_u P_b} \tag{19}$$

An unconfined explosion can be described by an enclosed explosion with a vent, and the pressure ratio P_0/P_b is approximately equal to 1 and E is:

$$E \approx \frac{\overline{M}_u T_b}{\overline{M}_b T_u} \tag{20}$$

Unburnt fuel in the tube is pushed to move by the flame front. Such moving speed of unburnt fuel cannot be ignored. The initial explosion speed S_I would affect the flame speed S_F by:

$$S_F = ES_T + S_I \tag{20}$$

The initial speed of unburnt fuel U is given in terms of the instantaneous flame front speed S_{FF} by [29]:

$$U = \frac{E-1}{E} S_{FF} \tag{21}$$

Before the explosion in the tube has reached detonation, increase in flame front speed is limited. For a thin enough flame sheet and short travel distance, $S_{FF} \approx S_F$:

$$S_F = E^2 S_T \tag{22}$$

Therefore, the flame propagation speed in explosion at a point depends on the turbulent burning speed and expansion ratio. It is difficult to estimate the turbulent speed, which depends on the geometry of explosion tube, structure, types of fuel gas and mixing ratio with air and burning environment.

From experimental observation on the explosion tube experiments above, for premixed fuel with constant expansion ratio, S_T changes with distance x. For flame due to explosion of premixed fuel such as methane (CH_4) [8] with adequate uniform concentration in the tube, S_T is assumed to be given in terms of two constants C_A and C_B,

$$S_T = \exp(C_A x + C_B) \tag{23}$$

From the expansion ratio of methane $E \approx 7.5$, the flame propagation speed in explosion can be simplified as:

$$S_F = E^2 \times \exp(C_A x + C_B) \tag{24}$$

or

$$S_F = 56.25 \times \exp(C_A x + C_B) \tag{25}$$

Putting S_F at different position x in Fig. 10 yields $C_A = 0.33\ m^{-1}$ and $C_B = -1.99$.

Flame propagation in deflagration experiment in an industrial scale piping of 25 m long and 0.254 diameter reported by Chatrathi et al. [10] was also used to justify equation (24). Fuels of equivalent ratio of 1 on propane (4.0%), ethylene (6.5%) and hydrogen (30%) with air were used with flame propagation speed at deflagration stage studied. Expansion ratios

were taken as 7.6 for propane (4.0%), 8.8 for ethylene (6.5%) and 5.7 for hydrogen (30%), in deriving expressions given by equation (24) with C_A and C_B shown in Table 4, with good values of γ^2. As shown in Fig. 11, equation (24) gives reasonably good fitting of the experimental data [10].

When fuel concentrations at upper and lower parts of the explosion tube are not distributed uniformly, flame development characteristics due to explosion will be affected by the tube wall. Unburnt fuel and air mixing is complicated, giving transient variations of fuel concentration along the tube, affected by space volume, and dimensions of the tube. Under such situations with turbulent flow, flame develops in a very complicated way. Simple analytical expression cannot be derived easily on the flame development.

For example, there are two chambers A and B in the 11 m long tube to give two zones of different fuel concentrations as in Fig. 2c. The flame speed is shown in Fig. 12. As the fuel concentration in the two zones A and B are different as in Fig. 2c, the flame developed upon explosion at different locations would have different fuel concentrations with sharp changes at the boundary between chambers A and B. The flame propagation would be affected by such sudden changes in fuel concentration.

As chamber A has a lower initial fuel concentration, flame developed with a slower speed. Flame speeds near to the ignition source rose with a slower rate. When the flame further developed and the fuel concentration at chamber B was higher, a faster flame speed was then observed. Upon burning up the air, flame speeds decreased at positions with higher fuel concentration. High explosion pressure pushed unburnt fuel to the tube end. With air supplied to hot fuel at the end, flame speed increased again. The phenomenon is very complicated and difficult to be described by simple analytical expression on flame speed at different positions. More detailed investigation is required for further studies in modelling flame propagation.

For single-zone experimental scenarios S1, S2 and S3, S_F at different x near to the closed end of the 25 m explosion tube are plotted in Fig. 13. As fuel at the closed end was used up without further supplies as in other experiments [8,10] shown in Figs. 10 and 11, flame did not propagate so fast. Fuel concentrations in scenario S3 were higher, giving higher S_F than scenarios S1 and S2 with lower fuel concentrations. But at 6 m, S_F reduced because of lower fuel concentrations.

Fuel concentrations in scenarios S1 and S2 near to the tube end are low, and so inadequate to support deflagration in the tube to give flame speed increased in exponent function. Equation (24) is then not appropriate to relate S_F with x.

For scenario S3 with LPG of expansion ratio E of 7.6, another equation similar to equation (24) is suggested:

$$S_F = 57.76 \times \exp(C_A x + C_B) \quad (26)$$

Putting S_F at different position x in Fig. 14 yields C_A = 0.12 m^{-1} and C_B = -0.41. In general, equation (24) can be used to study S_F at different positions x for deflagration in the explosion tube. However, for experiments with the fuel concentrations decreased largely upon consumption in explosion, S_F reduced and cannot be fitted by an exponent increasing function at different x. Appropriate values of expansion ratio and turbulent burning speed have to be used for better modeling of S_F. More experimental data are required to measure such values.

7. Conclusion

With the wider use of LPG vehicles, more accidental explosions are expected and in fact several big ones have been reported. Moreover, there are fuel reservoirs everywhere with limited safety provisions in developing countries. Motivated by such concerns, experimental studies on LPG explosion in a tube of 2.6 m diameter were carried out in the present study. Flame shape inside and outside the tube were captured by video cameras. With regard to flame propagation within a certain distance from the ignition point, the measured position of the flame front obeys an exponential law which can be derived using a very simple approach. The exponential law for flame front propagation is also consistent with the results reported in the literature.

Analytical study suggested that the flame propagation speed in explosion at a point depends on the turbulent burning speed and expansion ratio. For explosion in a tube with adequate gas concentration, flame propagation speed at different locations near to the ignition position can be fitted by a simple exponential function. However, greater deviations are expected for tubes with large variation of fuel concentration. Correction by measuring appropriate values of expansion ratio and turbulent burning speed is recommended.

Acknowledgements

The work described in this article was supported by a grant from the Research Grants Council of the Hong Kong Special Administrative Region for the project “A study on explosion hazards of clean refrigerant propane leaking from air-conditioning units in small commercial flats” (PolyU 152034/14E) with account number B-Q42U and National Natural Science Foundation of China (No. 51676051).

References

1. L. Wong, Updates on safety aspects on repair and maintenance of LPG vehicles, Chemical Safety Seminar organized by Occupational Safety and Health Council at Hong Kong Convention and Exhibition Center, 22 March 2016.
2. S. Chamberlain, M. Modarres, Compressed natural gas bus safety: A quantitative risk assessment, Risk Analysis, 25:2 (2005) 377-387.
3. Y. Huo, Y.W. Ng, W.K. Chow, A study on gas explosions in garages: LPG as fuel or for air-conditioner?, In: Heiselberg, P.K. (Ed.) CLIMA 2016 - Proceedings of the 12th REHVA World Congress: Volume 5, Aalborg, Denmark: Aalborg University, Department of Civil Engineering, 2016.
4. Yiu-wah Alexander Ng, Wan-ki Chow, Use of clean refrigerants and their potential fire hazards in Hong Kong, ASME-ATI-UIT 2015 Conference on Thermal Energy Systems: Production, Storage, Utilization and the Environment, 17-20 May, 2015, Napoli, Italy.
5. W.K. Chow, Any explosion risk for environmentally friendly refrigerants?, Invited talk, Chemical Safety Seminar organized by Occupational Safety and Health Council, Hong Kong Convention and Exhibition Center, 22 March 2016.
6. M.J. Sapko, E.S. Weiss, K.L. Cashdollar, I.A. Zlochower, Experimental mine and laboratory dust explosion research at NIOSH, Journal of Loss Prevention in the Process Industries, 13 (2000) 229-242.
7. K.L. Cashdollar, E.S. Weiss, S.P. Harteis, M.J. Sapko, Experimental study of the effect of LLEM explosions on various seals and other structures and objects, U.S.: National Institute for Occupational Safety and Health Pittsburgh Research Laboratory, 2007.
8. B.J. Lowesmith, C. Mumby, G. Hankinson, J.S. Puttock, Vented confined explosions involving methane/hydrogen mixtures, International Journal of Hydrogen Energy, 36 (2011) 2337-2343.
9. R. Hajossy, I. Morva, The optimum experimental design for reconstruction of flame-front propagation in a long pipe, Measurement Science and Technology, 9:1 (1998) 100-108.
10. K. Chatrathi, J.E. Going, B. Grandestaff, Flame propagation in industrial scale piping, Process Safety Progress, 20:4 (2001) 286-294.
11. V. Bychkov, A. Petchenko, V. Akkerman, L.E. Eriksson, Theory and modeling of accelerating flames in tubes, Physical Review, E 72 (2005) 046307: 1-10.
12. V. Akkerman, V. Bychkov, A. Petchenko, L.E. Eriksson, Accelerating flames in cylindrical tubes with nonslip at the walls, Combustion and Flame, 145 (2006) 206-219.
13. V. Akkerman, C.K. Law, V. Bychkov, L.E. Eriksson, Analysis of flame acceleration induced by wall friction in open tubes, Physics of Fluids, 22 (2010) 053606: 1-14.
14. Huahua Xiao, Qingsong Wang, Xiaobo Shen, Weiguang An, Qiangling Duan, Jinhua

Sun, An experimental study of premixed hydrogen/air flame propagation in a partially open duct. International Journal of Hydrogen Energy, 39 (2014) 6233-6241.

15. H. Hisken, G.A. Enstad, P. Middha, K. van Wingerden, Investigation of concentration effects on the flame acceleration in vented channels, Journal of Loss Prevention in the Process Industries, 36 (2015) 447-459.
16. Minggao Yu, Kai Zheng, Ligang Zheng, Tingxiang Chu, Pinkun Guo, Effects of hydrogen addition on propagation characteristics of premixed methane/air flames, Journal of Loss Prevention in the Process Industries, 34 (2015) 1-9.
17. Minggao Yu, Kai Zheng, Ligang Zheng, Tingxiang Chu, Pinkun Guo, Scale effects on premixed flame propagation of hydrogen/methane deflagration, International Journal of Hydrogen Energy, 40 (2015) 13121-13133.
18. Zhouquan Cai, Zhenmin Luo, Fangming Cheng, Experimental study on propagation characteristics of gas/coal dust explosion, Journal of China Coal Society, 34:7 (2009) 938-941. (In Chinese)
19. C.T. Johansen, G. Ciccarelli, Visualization of the unburned gas flow field ahead of an accelerating flame in an obstructed square channel, Combustion and Flame, 156 (2009) 405-416.
20. Jiasong Luo, Xiaolin Wei, Sen Li, Lixin Yu, Yu Zhang, Teng Li, Bo Li, Study on peak overpressure and flame propagation speed of gas deflagration in the tube with obstacles, Science China Technological Sciences, 53:7 (2010) 1847-1854.
21. B. Demirgok, H. Sezer, V. Akkerman, Flame acceleration due to wall friction: Accuracy and intrinsic limitations of the formulations, Modern Physics Letters B, 29 (2015) 1550205: 1-16.
22. R. Blanchard, D. Arndt, R. Gratz, M. Poli, S. Scheider, Explosions in closed pipes containing baffles and 90 degree bends, Journal of Loss Prevention in the Process Industries, 23 (2010) 253-259.
23. Sina Davazdah Emami, Meisam Rajabi, Che Rosmani Che Hassan, Mahar Diana A. Hamid, Rafiziana M. Kasmani, Mojtaba Mazangi, Experimental study on premixed hydrogen/air and hydrogen-methane/air mixtures explosion in 90 degrees bend pipeline, International Journal of Hydrogen Energy, 38 (2013) 14115-14120.
24. Sina Davazdah Emami, Siti Zubaidah Sulaiman, Rafiziana Md. Kasmani, Mahar Diana Hamid, Che Rosmani Che Hassan, Effect of pipe configurations on flame propagation of hydrocarbons-air and hydrogen-air mixtures in a constant volume, Journal of Loss Prevention in the Process Industries, 39 (2016) 141-151.
25. D.M. Valiev, V. Bychkov, V. Akkerman, L.E. Eriksson, C.K. Law, Quasi-steady stages in the process of premixed flame acceleration in narrow channels, Physics of Fluids, 25 (2013) 096101: 1-16.
26. Cheng Wang, Xinzhuang Dong, Jun Cao, Jianguo Ning, Experimental investigation of

flame acceleration and deflagration-to-detonation transition characteristics using coal gas and air mixture, Combustion Science and Technology, 187 (2015) 1805-1820.

27. Junfeng Wang, Jianming Wu, Yunlong Bai, Experimental research on the effects of South Africa's HS suppression system, China Safety Science Journal, 20:6 (2010) 63-68. (In Chinese)
28. J. Nagy, J.W. Conn, H.C. Verakis, Explosion development in a spherical vessel. Report of Investigations RI 7279, Pittsburgh, PA: U.S. Department of the Interior, Bureau of Mines, 1969.
29. M. Silvestrini, B. Genova, G. Parisi, F.J. Leon Trujillo, Flame acceleration and DDT run-up distance for smooth and obstacles filled tubes, Journal of Loss Prevention in the Process Industries, 21 (2008) 374-392.

Appendix: Mathematical Derivation

Fig. A1 shows flame propagation in an explosion tube with an open end, at time t and flame front position at x.

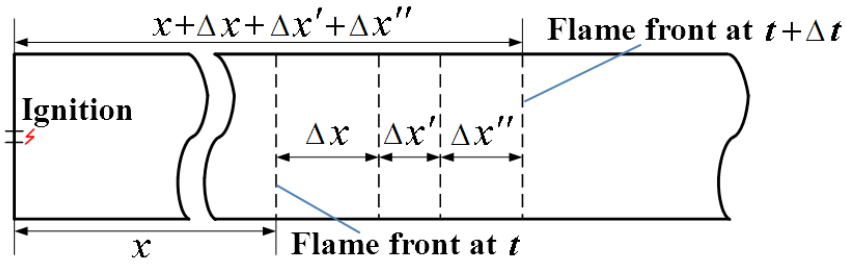

Fig. A1: Flame travel in tube with one end open

In time Δt, a mass of fuel Δm mixes with air. There are three contributions to the advancement of the flame front, attributable to chemical reaction, change in molar amounts, and thermal expansion. Let the corresponding displacements in flame front be Δx, $\Delta x'$ and $\Delta x''$, and the corresponding increase in flame volume be ΔV, $\Delta V'$ and $\Delta V''$. There are four components in the flame front speed S_F:

$$S_F = S_C + S_N + S_E + S_I \tag{A-1}$$

In the above equation, S_C is burning velocity, characteristic of the reactivity of the constituents and their heat-transfer properties, m/s, S_N is a velocity component due to change in the number of moles during the combustion process, m/s, S_E is gas-expansion velocity, due to thermal heating, m/s, S_I is the initial velocity, and the initial velocity $S_I = 0$ if the gas is taken at rest initially.

In Δt, flame front moves from x to $x+\Delta x$ due to chemical reaction. Change in number of moles Δn_u is given by:

$$\frac{\Delta V}{\Delta t} = \frac{\Re T_u}{p}\frac{\Delta n_u}{\Delta t} \tag{A-2}$$

In the above equation, $\Re$ is the universal gas constant, $\Re = 8.314$, J/(mol·K), T_u is the temperature of the unburnt gases, K, p is the pressure, Pa, and V is the volume, m^3.

As $\Delta V = A\Delta x$ and the planar area A of flame front is the cross-sectional area of tube, the burning speed $S_C = \Delta x/\Delta t$ becomes:

$$S_{\mathrm{C}} = \frac{\Re T_{\mathrm{u}}}{Ap}\frac{\Delta n_{\mathrm{u}}}{\Delta t} \tag{A-3}$$

Conservation of mass gives:

$$\Delta m = \overline{M}_{\mathrm{u}}\Delta n_{\mathrm{u}} = \overline{M}_{\mathrm{b}}\Delta n_{\mathrm{b}} \tag{A-4}$$

In the above equation, $\overline{M}_{\mathrm{u}}, \overline{M}_{\mathrm{b}}$ are the average molecular weights of the unburnt and burnt gases, respectively, g/mol, and Δn_{u}, Δn_{b} are the number of moles of unburnt and burnt gases, respectively, mol.

During time Δt, the incremental volume due to change in the number of moles is $\Delta V' = A\Delta x'$, applying the equation of state to this incremental volume:

$$\frac{\Delta V'}{\Delta t} = \frac{\Delta x + \Delta x'}{\Delta t}A - \frac{\Delta x}{\Delta t}A = \frac{\Re T_{\mathrm{u}}}{p}\frac{\Delta n_{\mathrm{b}}}{\Delta t} - \frac{\Re T_{\mathrm{u}}}{p}\frac{\Delta n_{\mathrm{u}}}{\Delta t} \tag{A-5}$$

The temperature is assumed not to change during the reaction. Putting equation (A-4) to equation (A-5), the velocity due to the mole volume change $S_{\mathrm{N}} = \Delta x'/\Delta t$ can be expressed as:

$$S_{\mathrm{N}} = \frac{\Re T_{\mathrm{u}}}{Ap}\left(1 - \frac{\overline{M}_{\mathrm{b}}}{\overline{M}_{\mathrm{u}}}\right)\frac{\Delta n_{\mathrm{b}}}{\Delta t} \tag{A-6}$$

Chemical reaction leads to change in mass Δm and temperature rise from T_{u} to T_{b} while thermal expansion gives $\Delta V'' = A\Delta x''$. As in equation (A-5),

$$\frac{\Delta V''}{\Delta t} = \frac{\Re}{p}\left(T_{\mathrm{b}} - T_{\mathrm{u}}\right)\frac{\Delta n_{\mathrm{b}}}{\Delta t} \tag{A-7}$$

The flame velocity caused by gas expansion $S_{\mathrm{E}} = \Delta x''/\Delta t$ can be expressed as:

$$S_{\mathrm{E}} = \frac{\Re}{Ap}\left(T_{\mathrm{b}} - T_{\mathrm{u}}\right)\frac{\Delta n_{\mathrm{b}}}{\Delta t} \tag{A-8}$$

Putting equations (A-3), (A-6), (A-8) and $S_{\mathrm{I}} = 0$ into equation (A-1), the flame speed becomes:

$$S_F = \underbrace{\frac{\Re T_u}{Ap}\frac{\overline{M}_b}{\overline{M}_u}\frac{\Delta n_b}{\Delta t}}_{S_C} + \underbrace{\frac{\Re T_u}{Ap}\left(1-\frac{\overline{M}_b}{\overline{M}_u}\right)\frac{\Delta n_b}{\Delta t}}_{S_N} + \underbrace{\frac{\Re}{Ap}\left(T_b - T_u\right)\frac{\Delta n_b}{\Delta t}}_{S_E} + \underbrace{0}_{S_I} = \frac{\Re T_b}{Ap}\frac{\Delta n_b}{\Delta t} \quad \text{(A-9)}$$

$\Delta n_b/\Delta t$ is present in S_F, S_C, S_N and S_E, so $\Delta n_b/\Delta t$ is the key factor for the flame speed model. This is reasonable as all contributions originate from combustion, quantified by the rate of gas consumption $\Delta n_b/\Delta t$.

As reviewed by Nagy et al. 1969 [A1], the amount of gas ignited (or entering the flame front per unit time per unit area) was postulated to be constant for a given pressure and temperature.

$$\frac{1}{A}\frac{\Delta V}{\Delta t} = k'_r \quad \text{(A-10)}$$

where k'_r is a constant having dimensions of velocity, m/s.

Experiments show that k'_r varies with the temperature and pressure of the unburnt gas. Correlation of these parameters by theory produces relatively complex equations. For most mixture of gases or powders, experiments have indicated that k'_r can be simply expressed as [A2-A6]:

$$k'_r = k_r\left(\frac{T}{T_r}\right)^{\alpha}\left(\frac{p_r}{p}\right)^{\beta} \quad \text{(A-11)}$$

where T_r is temperature at the reference level, 298K, p_r is pressure at the reference level, 1.01325×10^5Pa, k_r denotes the laminar burning velocity at reference conditions of pressure and temperature, m/s, α is an exponent indicating the dependence of the rate of reaction on temperature, and β is an exponent indicating the dependence of the rate of reaction on pressure.

Combining equations (A-2), (A-4) and (A-10) gives $\Delta n_b/\Delta t$ or dn_b/dt,

$$\frac{dn_b}{dt} = S_{Lr}\left(\frac{T}{T_r}\right)^{\alpha}\left(\frac{p_r}{p}\right)^{\beta}\frac{Ap}{RT}\frac{\overline{M}_u}{\overline{M}_b} \quad \text{(A-12)}$$

Putting equation (A-12) in equations (A-3), (A-6), (A-8) and equation (A-9) gives:

$$S_{\mathrm{C}} = S_{\mathrm{Lr}}\left(\frac{T}{T_{\mathrm{r}}}\right)^{\alpha}\left(\frac{p_{\mathrm{r}}}{p}\right)^{\beta} \tag{A-13}$$

$$S_{\mathrm{N}} = S_{\mathrm{Lr}}\left(\frac{T}{T_{\mathrm{r}}}\right)^{\alpha}\left(\frac{p_{\mathrm{r}}}{p}\right)^{\beta}\left(\frac{\overline{M}_{\mathrm{u}}}{\overline{M}_{\mathrm{b}}} - 1\right) \tag{A-14}$$

$$S_{\mathrm{E}} = S_{\mathrm{Lr}}\left(\frac{T}{T_{\mathrm{r}}}\right)^{\alpha}\left(\frac{p_{\mathrm{r}}}{p}\right)^{\beta}\frac{(T_{\mathrm{b}} - T)}{T}\frac{\overline{M}_{\mathrm{u}}}{\overline{M}_{\mathrm{b}}} \tag{A-15}$$

$$S_{\mathrm{F}} = S_{\mathrm{Lr}}\left(\frac{T}{T_{\mathrm{r}}}\right)^{\alpha}\left(\frac{p_{\mathrm{r}}}{p}\right)^{\beta}\frac{T_{\mathrm{b}}}{T}\frac{\overline{M}_{\mathrm{u}}}{\overline{M}_{\mathrm{b}}} \tag{A-16}$$

References

A1. J. Nagy, J.W. Conn, H.C. Verakis, Explosion development in a spherical vessel. Report of Investigations RI 7279, Pittsburgh, PA: U.S. Department of the Interior, Bureau of Mines, 1969.

A2. M. Metghalchlchi, Burning velocities of mixtures of air with methanol, isooctane, and indolene at high pressure and temperature, Combustion and Flame, 48 (1982) 191-210.

A3. A.E. Dahoe, L.P.H. de Goey, On the determination of the laminar burning velocity from closed vessel gas explosions, Journal of Loss Prevention in the Process Industries, 16:6 (2003) 457-478.

A4. A.E. Dahoe, Laminar burning velocities of hydrogen-air mixtures from closed vessel gas explosions, Journal of Loss Prevention in the Process Industries, 18 (2005) 152-166.

A5. K. van Wingerden, Simulation of dust explosions using a CFD-Code, Proceedings of the Seventh International Colloquium on Dust Explosion, Bergen, Norway, 1996, pp. 642-651.

A6. M. Silvestrini, B. Genova, F.J. Leon Trujillo, Correlations for flame speed and explosion overpressure of dust clouds inside industrial enclosures, Journal of Loss Prevention in the Process Industries, 21: 555-562, 2008.

Nomenclature

A : Flame surface area
E : Expansion ratio
k_r : Laminar burning velocity at reference conditions of pressure and temperature
k'_r : Constant having dimensions of velocity
m : Mass
m_u : Mass of fuel gas mixture
m_b : Mass of fuel gas product
$\overline{M}_u$: Average molecular weights of the unburnt gases
$\overline{M}_b$: Average molecular weights of the burnt gases
Δn_u : Number of moles of unburnt gases
Δn_b : Number of moles of burnt gases
p : Pressure
p_r : Pressure at the reference level
p_u : Pressure of fuel gas mixture
p_b : Pressure of fuel gas product
P_0 : Environmental atmospheric pressure
P_b : Pressure after explosion
r : Radius of flame surface in tube
r'_{rms} : Turbulence intensity
R : Radius of tube
$\Re$: Universal gas constant
S_u : Speed of fuel gas supply at the flame front
S_I : Initial velocity of the gases
S_C : Burning velocity
S_N : Velocity due to the mole volume change
S_E : Gas-expansion velocity
S_F : Flame front speed
S_L : Flame front speed in laminar flow
S_{Lr} : Reference speed
S_T : Flame surface motion velocity due to turbulence
S_{FF} : Instantaneous flame front speed
t : Time
T : Temperature
T_r : Temperature at the reference level
T_u : Temperature of the unburnt gases
T_b : Temperature of the burnt gases
V : Volume

V_u : Volume of fuel gas mixture
V_b : Volume of fuel gas product
x : Direction for flame propagation in tube
ρ_u : Density of fuel gas mixture
ρ_b : Density of fuel gas product
α : An exponent indicating the dependence of the rate of reaction on temperature
β : An exponent indicating the dependence of the rate of reaction on pressure
γ : Regression coefficient
C : Coefficient
C_A : Coefficient
C_B : Coefficient
K : Coefficient

Figure captions

Tables

Table 1: Recent experiments in explosion tube with diameter over 1 m

Authors	Cross-sectional area (m^2)	Tube length (m)	Research works
Sapko et al. (2000) [6]	11.2-13	76-195	1. Determined the conditions under which the laboratory tests well agreed with the full-scale tests. 2. Evaluated the explosion resistance characteristics of seals to separate non-ventilated, inactive workings from active workings of a mine.
Cashdollar et al. (2007) [7]	12-13	521	Studied the destruction of high pressure induced in coal mines.
Lowesmith et al. (2011) [8]	8.4	8.25	1. Assessed the effect of different hydrogen concentrations on the resulting explosion overpressures. 2. Studied the barrier effect in the explosion tube.
Hisken et al. (2015) [15]	1.44	6	Studied the explosion characteristics of propane-air gas with barrier in the tube.
Cai et al. (2009) [18]	7.2	658	Studied shock wave characteristics in gas and coal powder explosion.
	6.25	6	
	4.9	200	

Table 2: Experimental results and values of C_1 and C_2 from fitting

Experiment	Number	Tube length (m)	Chamber A		Chamber B		C_1 (m)	C_2 (1/s)	γ^2
			Length (m)	LPG ratio (%)	Length (m)	LPG ratio (%)			
	S1		1				0.3457	6.106	0.9876
	S2		2				0.00791	10.15164	0.9791
	S3		3				0.00065	13.05024	0.9669
	D1		2		5		0.03094	7.4324	0.8126
	D2		3		4		0.000012	10.57944	0.9678
	D3		4		4		0.00662	6.87641	0.8878
	D4		2		3		0.05451	4.36041	0.9903
	D5		3		4		0.00765	4.67554	0.9515

Table 3: Selected experimental results reported in literature

Experiment	Tube length (m)	Tube cross-sectional area (m^2)	Fuel	Barrier	C_1 (m)	C_2 (1/s)	γ^2
			CH_4	-	0.29388	6.13995	0.9803
			CH_4:H_2 mixture (80:20 by volume)	-	0.26735	7.23273	0.9789
			CH_4: H_2 mixture (50:50 by volume)	-	0.17258	14.66822	0.9593
			CH_4: H_2 mixture (80:20 by volume)	with pipes	0.0981	10.73399	0.9507
			CH_4: H_2 mixture (50:50 by volume)	with pipes	0.33524	10.85225	0.9761
Wang et al. (2010) [27]	200	4.9	CH_4	-	3.71327	4.03341	0.9822

Table 4: Fitted values from Chatrathi et al. (2001)

Combustion gas	C_A (m^{-1})	C_B	γ^2
4% Propane	0.18	-0.85	0.9852
6.5% Ethylene	0.20	-0.98	0.9688
30% Hydrogen	0.1313	1.72	0.9145

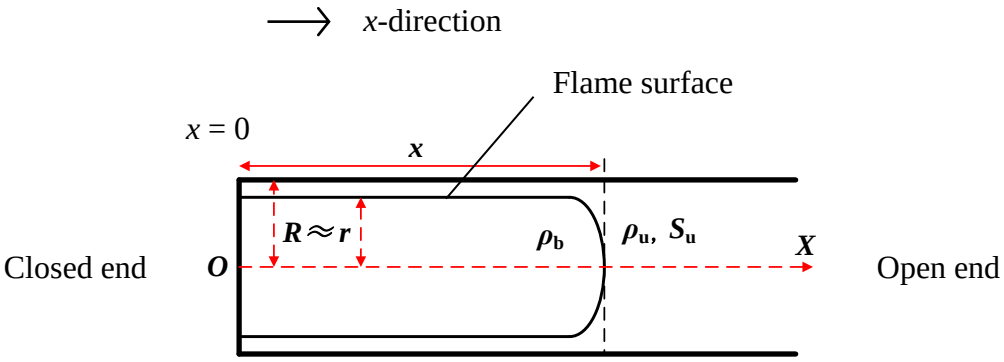

Fig. 1: Schematic diagram for flame propagation modelling

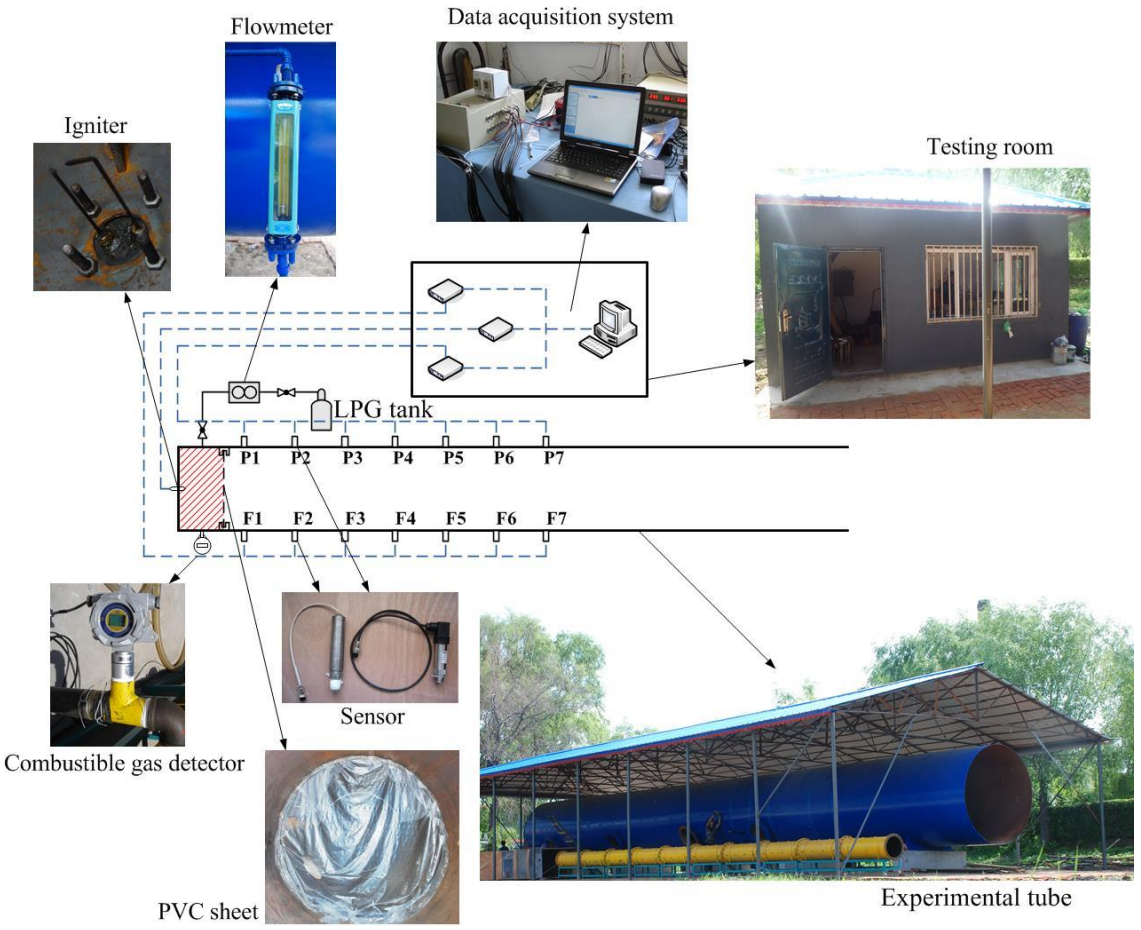

(a) Instrumentation

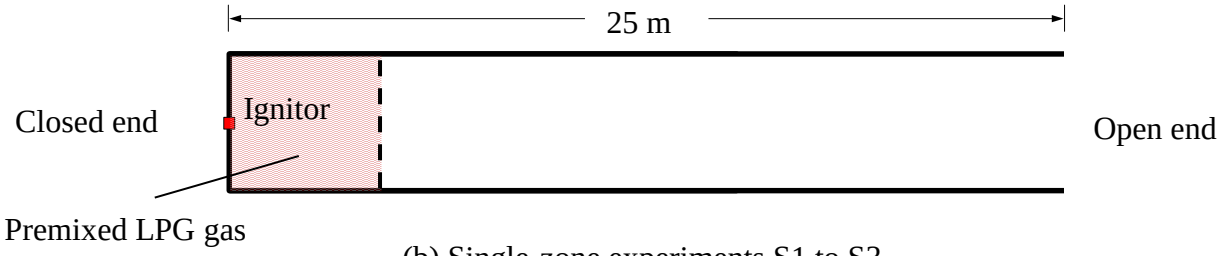

(b) Single-zone experiments S1 to S3

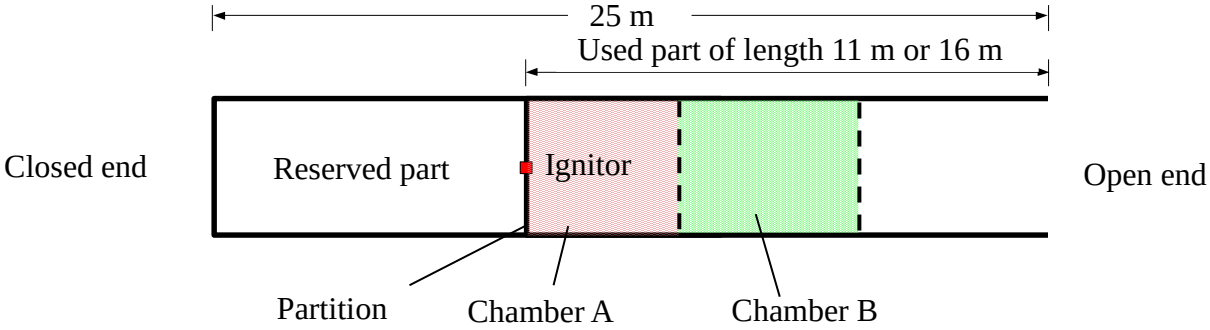

Partitioned the tube into two combustion chambers

(c) Two-zone experiments D1 to D5

Fig. 2: Details of the explosion experiment

(i) At 1.4 s (ii) At 1.65 s (iii) At 1.78 s (iv) At 1.98 s

(a) Tube of effective length 11 m (experiment D2)

(i) At 1.65 s (ii) At 1.75 s (iii) At 1.85 s (iv) At 1.95 s

(b) Tube of effective length 16 m (experiment D5)

Fig. 3: Side views of experiments showing flames beyond the open end of tube

(a) At 0.57 s (b) At 0.81 s (c) At 0.85 s

(d) At 0.89 s (e) At 0.98 s (f) At 1.02 s

Fig. 4: Flame pattern from the open end for effective tube length of 11 m (experiment D2)

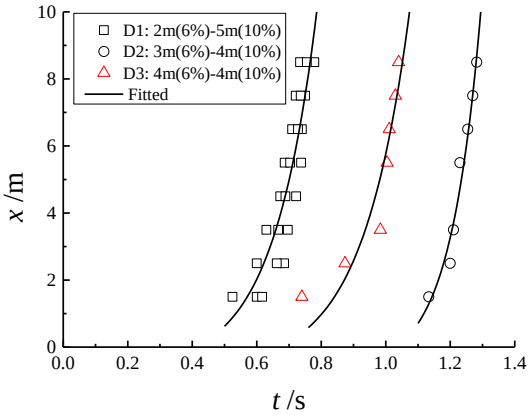

(a) 11 m tube length arrangement

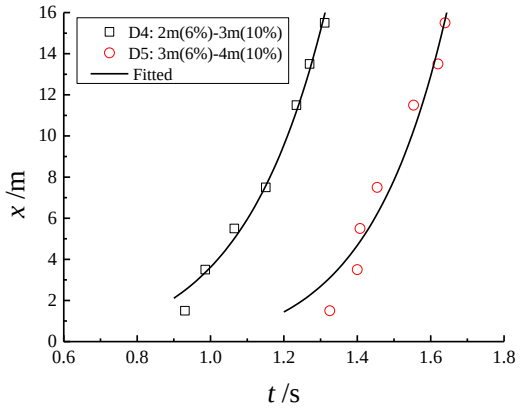

(b) 16 m tube length arrangement

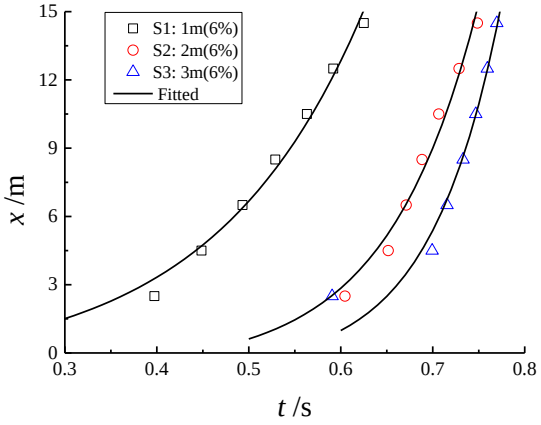

(c) 25 m tube length arrangement

Fig. 5: Flame fronts at different times

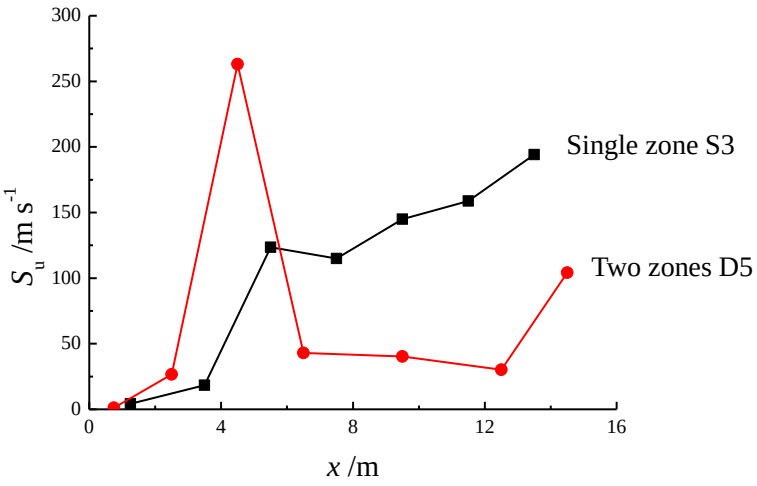

Fig. 6: Variation of flame speed at different positions

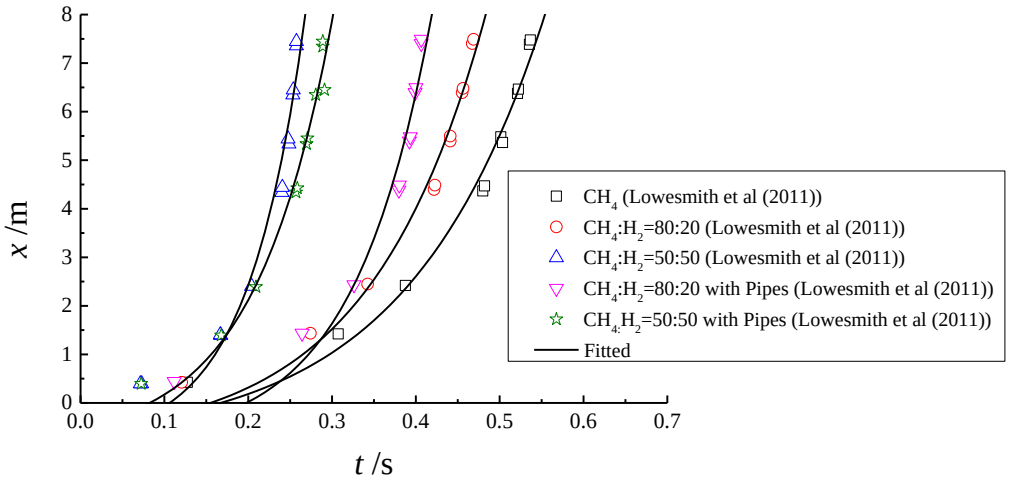

Fig. 7: Experimental results of 8-m long tube by Lowesmith et al. (2011)

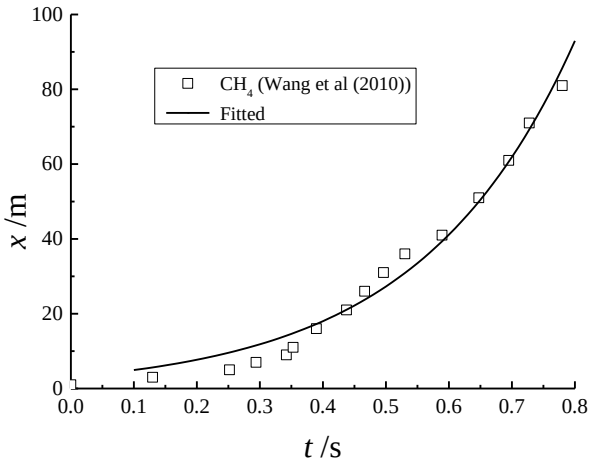

Fig. 8: Experimental results of 200-m long tube by Wang et al. (2010)

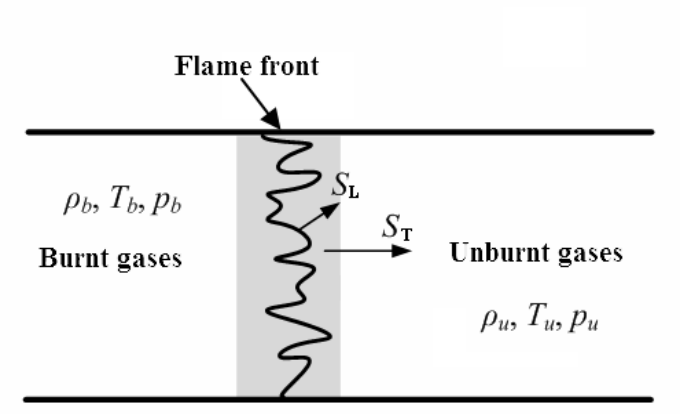

Fig. 9: Turbulent flow superposed on laminar flow in flame front in tube

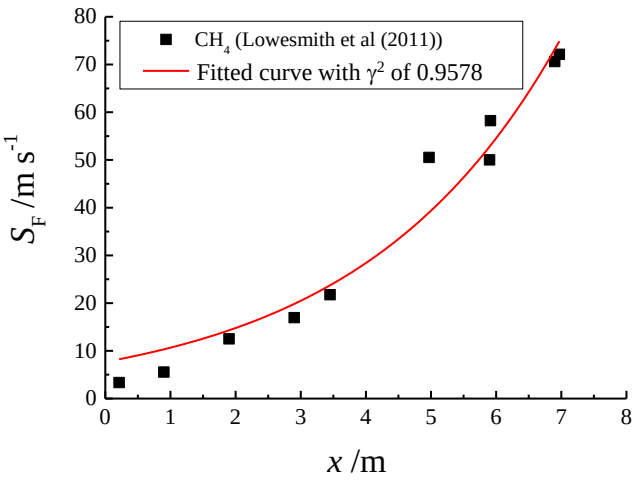

Fig. 10: Variation of flame speed at different positions

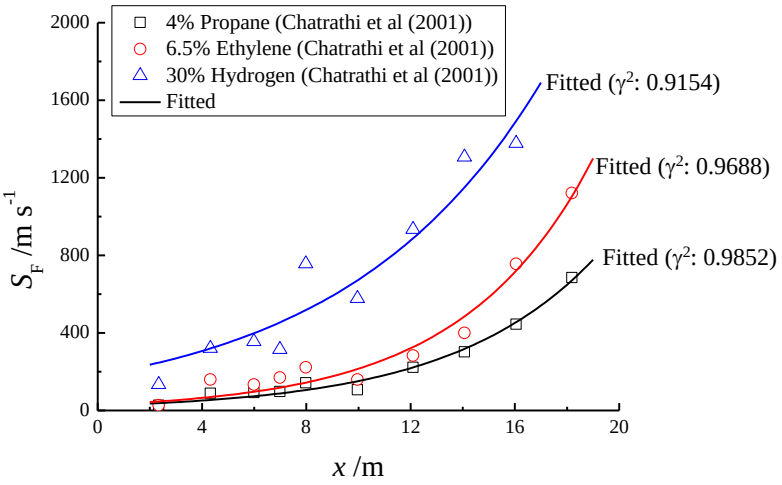

Fig. 11: Variation of flame speed at along an industrial scale pipe

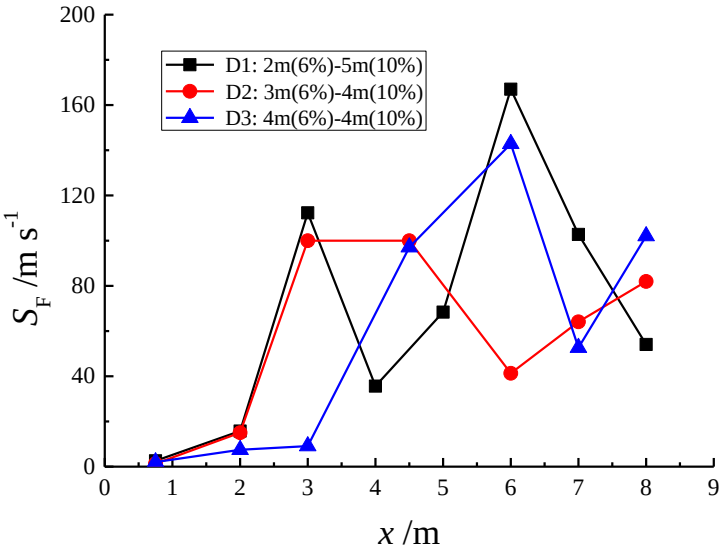

Fig. 12: Variation of flame speed at different positions in the 11 m tube length

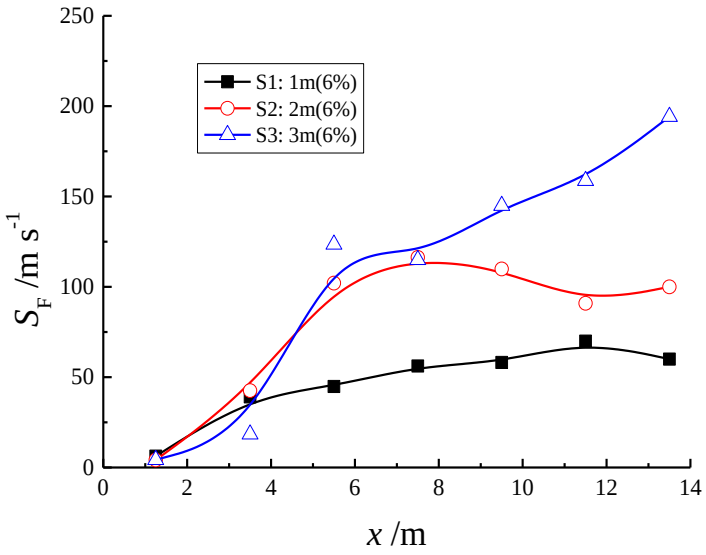

Fig. 13: Variation of flame speed along the 25 m tube length

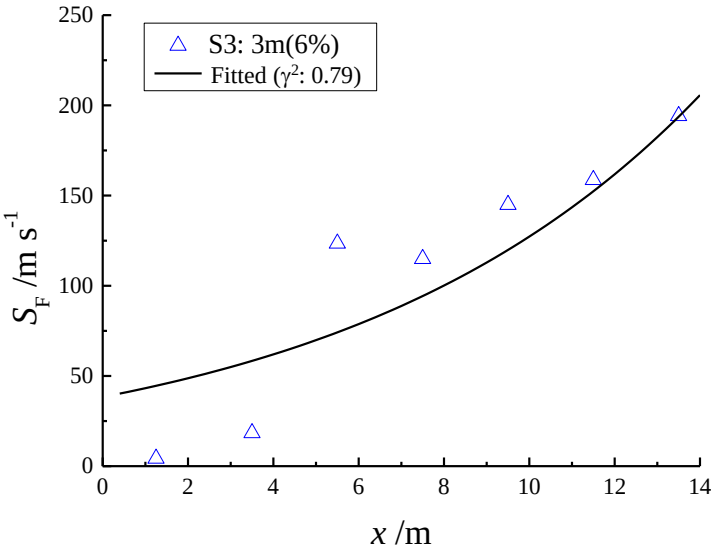

Fig. 14: Variation of flame speed at different positions of experiment S3